Noname manuscript No.
(will be inserted by the editor)

Dual-Phase Flow in Multilayered Porous Media

A Radial Composite Laplace Domain Approximation

Ana Luiza Mastbaum · **Ayla Bosso de Souza** ·
Jéssica Lailla Ferreira Bittencourt Neto · **Renan Vieira Bela** · **Abelardo Borges Barreto Jr**

Received: date / Accepted: date

Abstract The main purpose of this work is to present an interpretation method for injectivity test in a multilayer reservoir, based on new analytical solutions to the well pressure response. The developed formulation uses a radially composite reservoir approach and considers that the water front propagation may be approximated by a piston-like flow displacement. The reservoir is assumed to be laterally infinite and properties such as permeability and porosity may be different in each layer. The solutions were developed in the Laplace domain and then inverted to real domain using the Stehfest Algorithm. The proposed formulation was then validated by comparison with a numerical flow simulator. Results showed a good agreement between the numerical simulator and the analytical model. Also, a sensitivity study was done by comparing the results of different scenarios varying oil viscosities and injection flow rate to assess how these properties affect the pressure and pressure derivative profiles.

Keywords Well Testing · Injectivity Test · Laplace Domain · Multilayered Reservoir

Article Highlights

- Pressure response in injectivity test
- Multilayer and laterally infinite reservoir
- Validation with a flow simulator

1 Introduction

The injection of water into oil reservoirs in order to extract relevant information regarding the characteristics of the reservoir has become an interesting alternative to conventional well testing, given that it has many advantages. In addition to bringing

Ana Luiza Mastbaum
Mathematics Department, Pontifical Catholic University of Rio de Janeiro
E-mail: analuizamast@gmail.com

greater safety to the procedure the method helps to reduce CO_2 emissions to the environment, since there is no need to gas/oil flaring which happens in a conventional well testing. However, it brings a new parameter to the problem since the system changes from a single-phase flow to a two-phase flow.

Operationally, the conventional and injectivity tests are completely different, however from the injectivity well testing we have enough information to perform the pressure behavior analysis.

With this analysis it is possible to obtain different reservoir properties, according to what it is requested or necessary to the study of the reservoir (Neto et al., 2020a). The method consists of injecting water at a constant rate during a period of time. After that, the well is shut in and then it is possible to analyze the pressure curves to estimate properties of the reservoir.

Solutions for injectivity test in the real field applied to a single layer and a multilayer reservoir have already been developed (Bela et al., 2019). Moreover, there exist solutions in the Laplace domain to injectivity test in a single layer reservoir (Neto et al., 2020b). But, to the best of our knowledge, this is the first time a solution for two-phase flow in a multilayer reservoir developed in the Laplace domain is presented.

The pressure solution was obtained using a system of linear equations built in Laplace domain and brought to the real field using Stehfest's Algorithm (Stehfest, 1970) including the boundary and coupling conditions adopted to the scenario studied here. This work extends the single-layer solution developed by Neto et al. (2020b) to multilayer reservoirs and the behavior observed in the curves of pressure and pressure derivative was analyzed in different cases considering a variation of properties in the layers of the reservoir. Also a computational model was built to compare the results obtained.

This work is divided into 5 sections. After the introduction the conceptual model is presented, followed by the implemented mathematical model. Then, there is the results section, containing the different cases analyzed, and lastly the conclusion.

2 Conceptual Model

The formulation of the problem considers a reservoir with two layers both with two regions, where the outer radius is the same in both layers and there is no formation crossflow. The well is assumed to be at the center of a circular zone in a cylindrical model (Nie et al., 2012). In this geometry there is a radial change in the properties as it passes from region 1 to region 2.

A schematic illustration of the physical model is shown in Figures 1 and 2.

The external boundary is considered infinite acting. Region 1 represents the flooded zone and region 2 correspond to the oil region, both considered homogeneous, in addition the interface of the regions is flat and it has no thickness. The fluid mobility (k/μ) and compressibility are different on each side and each layer thicknesses are constant. Also there is no resistance to flow between the two reservoir regions.

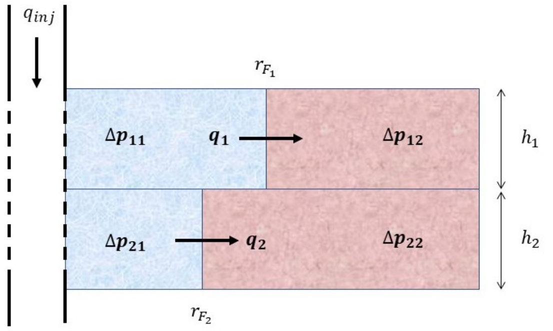

Fig. 1: Schematic illustration of the side view of the reservoir model

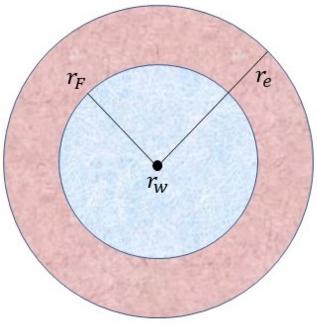

Fig. 2: Schematic illustration of the top view of the reservoir model

In the actual reservoir, a variation of properties around the wellbore at the interface of the regions can be observed due to the rock-fluid interaction. However those alterations were not considered in the model presented here.

For the mathematical formulation, the following hypotheses are considered:

1. Two-phase flow without interaction between the fluids and a piston-like fluid displacement in which the water pushes the oil completely.
2. Isothermal flow with negligible gravitational forces and ignoring the impact of capillary forces.
3. Same initial pressure (p_i) in all layers and small pressure gradients.
4. Reservoir is considered isotropic along each layer.
5. Single vertical injection well.
6. Constant flow rate during injection time.

7. Constant thickness (h) and porosity (ϕ) on each layer.
8. No flow considered in θ and z-directions.
9. The well is fully perforated along its extension.

3 Mathematical Formulation

Considering the reservoir model described in Section 2 a system of linear equations in Laplace domain is built to represent the differential equations of the water and oil phases, as well as the boundaries and coupling conditions.

The initial condition (IC) reflects the pressure distribution at the initial time along the reservoir. The internal boundary (IBC) indicates how the water is injected during the test, which, in this case, will be a constant flow rate. The external boundary condition (EBC) is relative to the flow behavior at the reservoir extreme limit. As it is considered a laterally infinite reservoir, that is, the reservoir boundaries, represented by the EBC, will not affect the well pressure response during the test time. The mathematical formulation was developed based on a consistent unit system.

Considering a piston-like fluid displacement, the fluid mobility ($\hat{\lambda}_i$), hydraulic diffusivity (η_i) and the derived fractional flow (f'_w) are defined by:

$$\hat{\lambda}_{ji} = \frac{k_j k_{rji}}{\phi \mu_{ji} c_t} \tag{1}$$

$$\eta_{ji} = \frac{k_j k_{rji}}{\mu_{ji}} \tag{2}$$

$$f'_w = \frac{1}{1 - S_{or} - S_{wi}} \tag{3}$$

The layer properties will be indicated by indices ji, where j represents the layer and i the region. Therefore, k_j is the layer permeability, k_{rji} is the relative permeability of the fluid.

Using the Buckley-Leverett formulation (Buckley and Leverett, 1942), the water front radius (r_F) is defined by:

$$r_{Fj}(t) = \sqrt{(r_w)^2 + \frac{v_{inj_j}(t)}{24\phi h_j} f'_w} \tag{4}$$

where v_{inj_j} is the water volume injected into each layer.

$$v_{inj_j}(t) = \int_0^t q_{inj}(t')\,dt' \tag{5}$$

Thus, the following equations model the problem:
Region 1:
PDE:

$$\frac{\partial}{\partial r}\left(r \frac{\partial p_{j1}(r,t)}{\partial r}\right) = \frac{1}{\eta_{j1}} \frac{\partial p_{j1}(r,t)}{\partial t} \tag{6}$$

IC:

$$p_{j1}(r,t) = p_i \tag{7}$$

IBC:

$$q_{j1} = -2\pi\hat{\lambda}_{j1}h_j\left(r\frac{\partial p_{j1}(r,t)}{\partial r}\right)\bigg|_{r=r_w} \tag{8}$$

Region 2:
PDE:

$$\frac{\partial}{\partial r}\left(r\frac{\partial p_{j2}(r,t)}{\partial r}\right) = \frac{1}{\eta_{j2}}\frac{\partial p_{j2}(r,t)}{\partial t} \tag{9}$$

IC:

$$p_{j2}(r,t) = p_i \tag{10}$$

EBC:

$$\lim_{r\to\infty} p_{j2}(r,t) = 0 \tag{11}$$

The relationship between the regions and layers are expressed by the coupling conditions. The pressure and flow-rate equalities in each region at the interface between them, that is, at the water front radius (r_F), represent the coupling conditions by region (CCR) (Nie et al., 2011). This condition is defined as:

CCR:

$$\begin{cases} \Delta p_{j1}(r_{Fj},t) = \Delta p_{j2}(r_{Fj},t) \\ q_{j1}(r_{Fj},t) = q_{j2}(r_{Fj},t) \end{cases} \tag{12}$$

Applying Darcy's Law to compute the flow-rate in each region:

$$2\pi\hat{\lambda}_{j1}h_j\left(r\frac{\partial p_{j1}}{\partial r}\right)\bigg|_{r=r_{Fj}} = 2\pi\hat{\lambda}_{j2}h_j\left(r\frac{\partial p_{j2}}{\partial r}\right)\bigg|_{r=r_{Fj}} \tag{13}$$

As one can see, both, water and oil rates are considered the same, however it is only an approximation that can be applied in a piston-like problem.

Therefore,

$$\left(r\frac{\partial p_{j1}}{\partial r}\right)\bigg|_{r=r_{Fj}} = \frac{\hat{\lambda}_{j2}}{\hat{\lambda}_{j1}}\left(r\frac{\partial p_{j2}}{\partial r}\right)\bigg|_{r=r_{Fj}} \tag{14}$$

Equations (13) and (14) refer only to the flow-rate CCR (12).

Since the considered reservoir model assumes that layers have no connection to each other except by the wellbore, the coupling condition by layers (CCL) is given by the pressure equality and the principle of mass conservation at this same point as shown below:

CCL:

$$\begin{cases} \Delta p_{j,1}(r_w,t) = \Delta p_{j+1,1}(r_w,t) \\ q_{inj} = \sum\limits_{j=1}^{n} q_{j1}(r_w,t) \end{cases} \tag{15}$$

Bringing the equations to Laplace domain:

Region 1:
PDE:

$$\frac{1}{r}\frac{\partial}{\partial r}\left(r\frac{\partial \bar{p}_{j1}}{\partial r}\right) = \frac{1}{\eta_{j1}}(u\bar{p}_{j1}(r,u) - p_{j1}(r,t=0)) \tag{16}$$

Applying the Laplace transform in equations (6) to (11) and applying the IC (given by equations (7) and (10)), the following Ordinary Differential Equation for Region 1 is obtained:

ODE:

$$\frac{\partial^2 \bar{p}_{j1}(r,u)}{\partial r^2}+\frac{1}{r}\frac{\partial \bar{p}_{j1}(r,u)}{\partial r}=\frac{1}{\eta_{j1}}\left(u\bar{p}_{j1}(r,u)-p_i\right) \tag{17}$$

IBC:

$$\left(r\frac{\partial \bar{p}_{j1}(r,t)}{\partial r}\right)\bigg|_{r=r_w}=\frac{-2\hat{\lambda}_{j1}h_j}{q_{j1}}\frac{1}{u} \tag{18}$$

Region 2:

ODE:

$$\frac{\partial^2 \bar{p}_{j2}(r,u)}{\partial r^2}+\frac{1}{r}\frac{\partial \bar{p}_{j2}(r,u)}{\partial r}=\frac{1}{\eta_{j2}}\left(u\bar{p}_{j2}(r,u)-p_i\right) \tag{19}$$

EBC:

$$\lim_{r\to\infty}\bar{p}_{j2}(r,u)=0 \tag{20}$$

The pressure change in Laplace domain may be defined as $\Delta\bar{p}(r,u)=p_i-\bar{p}(r,u)$ and $\frac{\partial\bar{p}}{\partial r}=-\frac{\partial\Delta\bar{p}}{\partial r}$. Thus, applying this definition for pressure change in equations (16) to (20), the following equations are obtained:

Region 1:

ODE:

$$\frac{\partial^2\Delta\bar{p}_{j1}}{\partial r^2}+\frac{1}{r}\frac{\partial^2\Delta\bar{p}_{j1}}{\partial r}-\frac{u}{\eta_{j1}}\Delta\bar{p}_{j1}=0 \tag{21}$$

IBC:

$$\left(r\frac{\partial\Delta\bar{p}_{j1}}{\partial r}\right)\bigg|_{r=r_w}=\frac{-q_{j1}}{2\pi\hat{\lambda}_{j1}h_j}\frac{1}{u} \tag{22}$$

Region 2:

ODE:

$$\frac{\partial^2\Delta\bar{p}_{j2}}{\partial r^2}+\frac{1}{r}\frac{\partial^2\Delta\bar{p}_{j2}}{\partial r}-\frac{u}{\eta_{j2}}\Delta\bar{p}_{j2}=0 \tag{23}$$

EBC:

$$\lim_{r\to\infty}\Delta\bar{p}_{j2}(r,u)=0 \tag{24}$$

Besides that, the coupling conditions in the Laplace domain are shown as:

CCR:

$$\begin{cases}\Delta\bar{p}_{j1}(r_{Fj},t)=\Delta\bar{p}_{j2}(r_{Fj},t)\\ \left(r\frac{\partial\Delta\bar{p}_{j1}}{\partial r}\right)\Big|_{r=r_{Fj}}=\frac{\hat{\lambda}_{j2}}{\hat{\lambda}_{j1}}\left(r\frac{\partial\Delta\bar{p}_{j2}}{\partial r}\right)\Big|_{r=r_{Fj}}\end{cases} \tag{25}$$

CCL:

$$\begin{cases}\Delta\bar{p}_{j,1}(r_w,t)=\Delta\bar{p}_{j+1,1}(r_w,t)\\ \frac{q_{inj}}{2\pi u\sum\limits_{j=1}^{n}\hat{\lambda}_{j1}h_j}=-\sum\limits_{j=1}^{n}\left(\frac{r\partial\Delta\bar{p}_{j1}}{\partial r}\right)\Big|_{r=r_w}\end{cases} \tag{26}$$

The pressure solution for any layer j and region i in Laplace domain is:

$$\Delta \bar{p}_{ji} = A_{ji} K_0 \left(r \sqrt{\frac{u}{\eta_{fj}}} \right) + B_{ji} I_0 \left(r \sqrt{\frac{u}{\eta_{fj}}} \right) \tag{27}$$

where A_{ji} and B_{ji} are coefficients to be determined. It is also known by the Bessel functions properties (Abramowitz and Stegun, 1964) that:

$$\lim_{r \to \infty} K_0(r) = 0 \tag{28}$$

$$\lim_{r \to \infty} I_0(r) = \infty \tag{29}$$

Thus, to satisfy the external boundary condition of Region 2 given by equation (24), B_{j2} must be zero. Consequently, the pressure solution for $i = 2$ is:

$$\Delta \bar{p}_{j2} = A_{j2} K_0 \left(r \sqrt{\frac{u}{\eta_{j2}}} \right) \tag{30}$$

By the IBC (22) and the flow-rate CCL (26):

$$\sum_{j=1}^{n} \left(r \frac{\partial \Delta \bar{p}_{j1}}{\partial r} \right) \Bigg|_{r=r_w} = - \frac{q_{inj}}{2\pi \sum\limits_{j=1}^{n} (\hat{\lambda}_{j1} h_j)} \frac{1}{u} \tag{31}$$

Thus, deriving the equation (27) with respect to $r = r_w$ may be combined with equation (31):

$$\sum_{j=1}^{n} \left(A_{j1} K_1 \left(r_w \sqrt{\frac{u}{\eta_{j1}}} \right) - B_{j1} I_1 \left(r_w \sqrt{\frac{u}{\eta_{j1}}} \right) \right) = \frac{1}{r_w \sqrt{\frac{u}{\eta_{j1}}}} \frac{q_{inj}}{2\pi \sum\limits_{j=1}^{n} (\hat{\lambda}_{j1} h_j)} \frac{1}{u} \tag{32}$$

Replacing the pressure solutions for Region 1 (27) in the corresponding CCL (26):

$$A_{11} K_0 \left(r_w \sqrt{\frac{u}{\eta_{j1}}} \right) + B_{11} I_0 \left(r_w \sqrt{\frac{u}{\eta_{j1}}} \right) = A_{21} K_0 \left(r_w \sqrt{\frac{u}{\eta_{j1}}} \right) + B_{21} I_0 \left(r_w \sqrt{\frac{u}{\eta_{j1}}} \right) \tag{33}$$

On the other hand, from equations (25) and (27), the following expression for the flow-rate CCR is obtained:

$$A_{j1} K_1 \left(r_{Fj} \sqrt{\frac{u}{\eta_{j1}}} \right) - B_{j1} I_1 \left(r_{Fj} \sqrt{\frac{u}{\eta_{j1}}} \right) = \frac{\hat{\lambda}_{j2}}{\hat{\lambda}_{j1}} \sqrt{\frac{\eta_{j1}}{\eta_{j2}}} A_{j2} K_1 \left(r_{Fj} \sqrt{\frac{u}{\eta_{j2}}} \right) \tag{34}$$

The last condition to be applied to this model is the pressure CCR (25). Therefore, combining the pressure solutions (27) and (30):

$$A_{j1} K_0 \left(r_{Fj} \sqrt{\frac{u}{\eta_{j1}}} \right) + B_{j1} I_0 \left(r_{Fj} \sqrt{\frac{u}{\eta_{j1}}} \right) = A_{j2} K_0 \left(r_{Fj} \sqrt{\frac{u}{\eta_{j2}}} \right) \tag{35}$$

The equations of hydraulic diffusivity, boundary conditions and coupling conditions of each region and layer provide a linear system that models this problem in the Laplace domain. The following equality represents this system:

$$M \begin{bmatrix} A_{11} \\ B_{11} \\ A_{12} \\ A_{21} \\ B_{21} \\ A_{22} \end{bmatrix} = \begin{bmatrix} \frac{1}{r_w \sqrt{\frac{u}{\eta_{w1}}}} \frac{q_{inj}}{2\pi \sum\limits_{j=1}^{2} (\hat{\lambda}_{j1} h_j)} \frac{1}{u} \\ 0 \\ 0 \\ 0 \\ 0 \\ 0 \end{bmatrix} \tag{36}$$

Where M is a linear system in matrix form composed of equations (32), (33), (34) and (35). Equation (32) represents the coefficients of the well pressure equation. Equation (33) expresses the coupling condition between layers and equations (34) and (35) express, respectively, the flow-rate and pressure coupling conditions between regions of both layers.

For a better understanding, the matrix M was divided into two parts, as shown below. The first part consists of its first three columns and the second one by its last three.

$$\begin{vmatrix} K_1\left(r_w\sqrt{\frac{u}{\eta_{w1}}}\right) & -I_1\left(r_w\sqrt{\frac{u}{\eta_{w1}}}\right) & 0 \\ K_0\left(r_w\sqrt{\frac{u}{\eta_{w1}}}\right) & I_0\left(r_w\sqrt{\frac{u}{\eta_{w1}}}\right) & 0 \\ K_1\left(r_{F1}\sqrt{\frac{u}{\eta_{w1}}}\right) & -I_1\left(r_{F1}\sqrt{\frac{u}{\eta_{w1}}}\right) & -\frac{\hat{\lambda}_{o1}}{\hat{\lambda}_{w1}}\sqrt{\frac{\eta_{w1}}{\eta_{o1}}} K_1\left(r_{F1}\sqrt{\frac{u}{\eta_{o1}}}\right) \\ K_0\left(r_{F1}\sqrt{\frac{u}{\eta_{w1}}}\right) & I_0\left(r_{F1}\sqrt{\frac{u}{\eta_{w1}}}\right) & -K_0\left(r_{F1}\sqrt{\frac{u}{\eta_{o1}}}\right) \\ 0 & 0 & 0 \\ 0 & 0 & 0 \end{vmatrix} \tag{37}$$

Thus, the last three columns of matrix M are represented by:

$$\begin{vmatrix} 0 & 0 & 0 \\ -K_0\left(r_w\sqrt{\frac{u}{\eta_{w2}}}\right) & -I_0\left(r_w\sqrt{\frac{u}{\eta_{w2}}}\right) & 0 \\ 0 & 0 & 0 \\ 0 & 0 & 0 \\ K_1\left(r_{F2}\sqrt{\frac{u}{\eta_{w2}}}\right) & -I_1\left(r_{F2}\sqrt{\frac{u}{\eta_{w2}}}\right) & -\frac{\hat{\lambda}_{o2}}{\hat{\lambda}_{w2}}\sqrt{\frac{\eta_{w2}}{\eta_{o2}}}K_1\left(r_{F2}\sqrt{\frac{u}{\eta_{o2}}}\right) \\ K_0\left(r_{F2}\sqrt{\frac{u}{\eta_{w2}}}\right) & I_0\left(r_{F2}\sqrt{\frac{u}{\eta_{w2}}}\right) & -K_0\left(r_{F2}\sqrt{\frac{u}{\eta_{o2}}}\right) \end{vmatrix} \tag{38}$$

Therefore, once the coefficients A_{11} and B_{11} were determined, it is concluded that, in Laplace domain, the well pressure solution is calculated by:

$$\Delta \bar{p}_{wf} = A_{11}K_0\left(r_w\sqrt{\frac{u}{\eta_{w1}}}\right) + B_{11}I_0\left(r_w\sqrt{\frac{u}{\eta_{w1}}}\right) \tag{39}$$

The well pressure profile given by equation (39) is then converted to real domain through Stehfest Algorithm (Stehfest, 1970).

4 Results

The accuracy of the analytical model detailed in Section 2 was determined by comparison with a commercial flow simulator (von Hohendorff Filho, 2004). The curves of pressure (ΔP) and pressure derivative with respect to the natural logarithm of time ($\Delta P'$) were plotted on log-log graphs functions of time. After the proposed solution was validated, a sensitivity study was performed, evaluating the influence of oil viscosity and injection flow-rate in the computed pressure response.

4.1 Model Validation

The endpoint mobility ratio is a ratio between the mobility of the fluids under discussion. It is a critical factor to influence flooding efficiency of the water in the reservoir. When the endpoint mobility ratio is greater than one, it means the water is more mobile than oil. Otherwise, it means the water is less mobile than oil, leading to a better sweep efficiency. Thus the mobility ratio is defined by:

$$\hat{M} = \frac{\hat{\lambda}_w}{\hat{\lambda}_o} = \frac{\mu_o}{\mu_w} \tag{40}$$

The results are divided in two cases, considering different mobility ratios between the fluids. The reservoir properties for both cases as well as the injection flow-rate are

Table 1: Input data for both cases

Parameter	Value	Units
q_{inj}	800	m³/day
k_1	125	mD
k_2	250	mD
h_1	15	m
h_2	15	m
ϕ_1	0.25	fraction
ϕ_2	0.25	fraction

Table 2: Fluid properties in each case

Case	μ_o (cP)	μ_w (cP)	$\hat{M}$
1	5.0	0.5	10
2	0.2		0.4

shown in Table 1. Meanwhile, the fluid viscosities for Cases 1 and 2 can be seen in Table 2. Also, it was considered a 96-hour flow period on both cases.

In Case 1, a 5 cP oil viscosity was tested, leading to a high mobility ratio and a better movement of the water, although not a great sweep efficiency in moving the oil along the radius of the reservoir. In Case 2, a lower oil viscosity was tested, leading to a mobility ratio lower than in Case 1 and consequently a better scenario to the sweep efficiency.

Figures 3 and 4 show the pressure and derivatives curves considering both the analytical solution and numerical data. A slight deviation between the curves at the short time can be observed due to the simulation grid refinement causing this line spacing can be observed. Besides that, in both cases it is possible to notice the proximity of the results showing a good agreement between the models.

In addition, this refinement problem appears to be more sensitive in Case 1, even for a long time. It can be explained by the water front behavior, i.e., piston-like and due to its mobility ratio, since it is higher than one and greater than Case 2, leading to a more unstable displacement.

It is also observed that the derivative starts at a certain level and then stabilizes at another one, which is the same for both cases, even though the oil viscosity is different. This can be explained by the fact that, in an injectivity test, the first level of the pressure derivative curve represents the oil mobility, while the second represents the water mobility. Thus, since the properties of the injected water are the same for Cases 1 and 2, the second derivative level is expected to be the same in both graphs.

4.2 Sensitivity Analysis

In order to analyze the proposed solution with different scenarios, the pressure and pressure derivative over time were plotted, in five different oil viscosities (maintaining the injection rate at 1400 m^3/day) as shown in Figure 5.

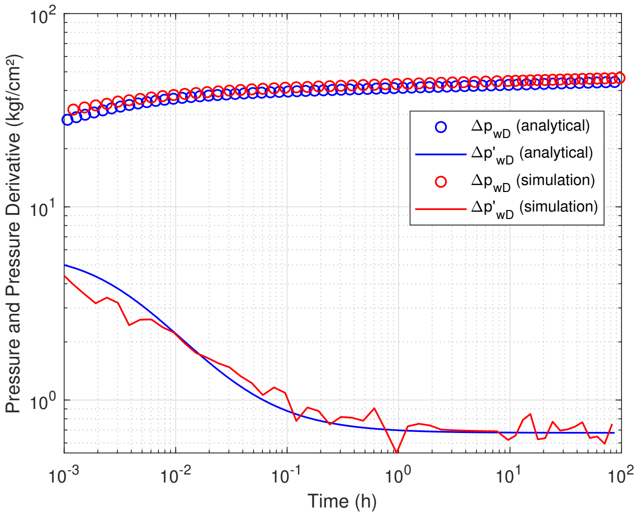

Fig. 3: Pressure and Pressure Derivative data for Case 1

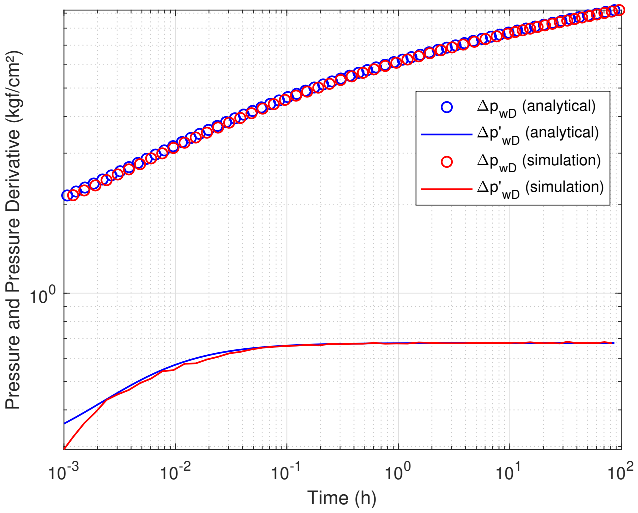

Fig. 4: Pressure and Pressure Derivative data for Case 2

The pressure derivatives for different oil viscosities in Figure 5 converge to the same level, as well as Figures 3 and 4. The reason behind this behavior is the same as mentioned in Section 4.1. As the oil viscosities are different for each curve and the first level of the pressure derivative curves represents the oil mobility, their initial level are not the same. However, as the properties of the injected water remain the same, the second level of all curves converge to a single threshold.

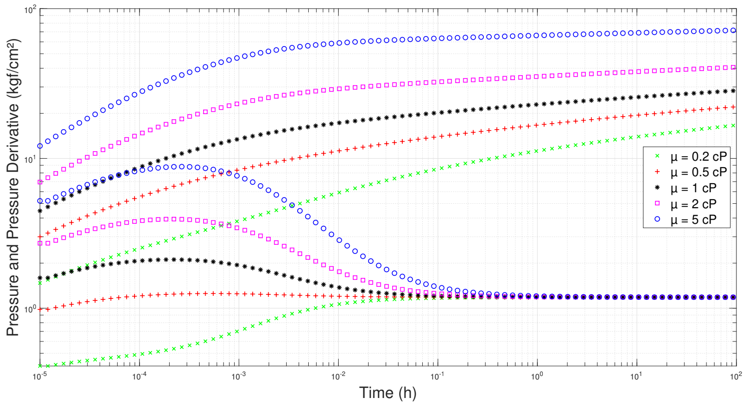

Fig. 5: Pressure and Pressure Derivative for different oil viscosities

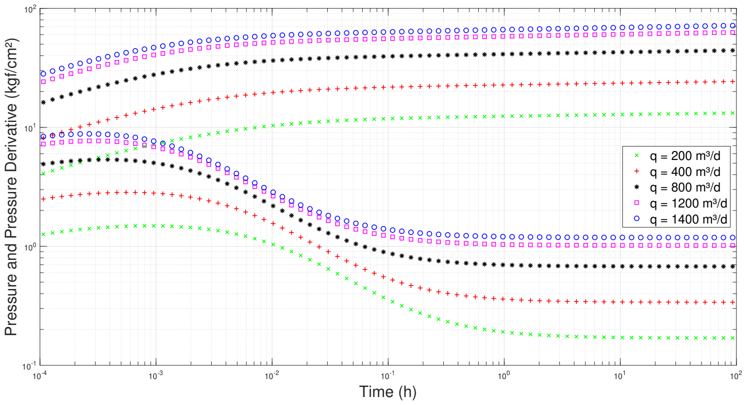

Fig. 6: Pressure and Pressure Derivative for different injection flow-rates

It is also possible to notice that the pressure curves rise as the oil viscosity increases. This is due to the fact that the higher the oil viscosity, the more distant it is from the water viscosity and therefore it departs from the 0.5 cP level. When oil and water viscosities are the same, pressure derivative remains constant during the entire test, since there is no difference between fluid mobilities.

Figure 6 displays the variation of injection rate maintaining the same oil viscosity as Case 1. Figure 7, on the other hand, enables easy visualization of the difference between the behavior of each scenario, once it shows the normalized pressure and pressure derivative data. The normalized pressure is given by each pressure divided by its injection rate versus time. Thus, pressure derivative is also normalized by the injection flow-rate.

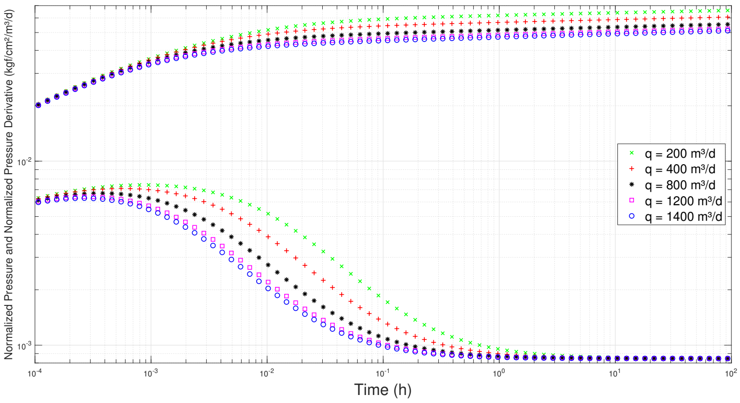

Fig. 7: Normalized Pressure and Pressure Derivative for different injection flow-rates

The decrease of the derivative pressure curves indicates the transition region between the oil properties region and the water properties region. Thus, looking at those same curves in Figure 7, it is noticed that as the injection flow-rate decreases it takes longer to reach the water level. The opposite occurs as the injection flow-rate increases. This is due to the fact that, with a lower injection rate, it takes longer for the water bank around the wellbore to become relevant, which means that pressure change will reflect water properties. However, considering the normalized pressure derivative data, all curves achieve the same level once the transition is over.

5 Conclusion

Based on the solution for pressure change during injectivity tests in single-layer reservoir, it was possible to develop a formulation to a multilayer reservoir. The proposed multilayer solution uses coupling conditions between layers and between regions to build the linear system that must be solved to determine the pressure change.

The comparison between the numerical model and the analytical model developed in this work shows the proximity of the results and accuracy of the solution, once both tested cases obtained a good agreement with the numerical simulator.

The sensitivity study was done comparing the results considering different oil viscosities and injection flow-rates. From this sensitivity study, it was possible to notice how these parameters influence the pressure response and pressure derivative.

Thereby, this work presents a new and accurate solution for pressure response during a water injection well testing in a way that is possible to evaluate the wellbore pressure response.

Although the work was based on a reservoir with only two layers, the presented solution may be extended to an arbitrary number of layers. This interpretation was possible considering an infinite reservoir with the boundary conditions not affecting the pressure behavior. However the model can be adapted to different boundary conditions, for that the definition made on EBC (11) must be modified.

Acknowledgements Authors are grateful to Petrobras for partially sponsoring this research. This study was financed in part by the Coordenação de Aperfeiçoamento de Pessoal de Nível Superior - Brasil (CAPES) - Finance Code 001.

Declarations

Funding

Partial financial support was received from Petrobras. Also this work was partially supported by the Coordenação de Aperfeiçoamento de Pessoal de Nível Superior - Brasil (CAPES) - Finance Code 001.

Conflicts of interest/Competing interests

The authors have no conflicts of interest to declare that are relevant to the content of this article.

Availability of Data and Materials

This work is theoretical and does not contain any real field data.

Code Availability

Not Aplicable.

Author Contributions

All authors contributed to the study conception and design. Material preparation, data collection and analysis were performed by Ana Luiza Mastbaum and Ayla Bosso de Souza. The research was supervised by Abelardo Borges Barreto Jr. All authors read and approved the final manuscript.

Nomenclature

$\bar{p}$	pressure in Laplace domain
η_{ji}	hydraulic diffusivity of the fluid in region i and layer j
$\hat{\lambda}_i$	fluid mobility of the fluid f, mD/cP
$\hat{M}$	mobility ratio, fraction
μ_i	viscosity of the fluid in region i, cP
ϕ	porosity, fraction
f_s'	fractional flow derivative
h_j	layer thickness, m
I_v	modified Bessel function of first kind and order v
k_j	layer permeability, mD
K_v	modified Bessel function of second kind and order v
k_{ri}	relative permeability of the fluid in region i, mD
p_i	initial pressure, kgf/cm^2
p_j	layer pressure, kgf/cm^3
p_w	bottom-hole pressure, kgf/cm^2
q_i	flow-rate of the fluid in region i, m^3/day
q_{inj}	injection rate, m^3/day

r_w	wellbore radius, m
r_{Fj}	water front radius in layer j, m
S_{or}	residual oil saturation, fraction
S_{wi}	initial water saturation, fraction
t	time, hrs
v_{inj_j}	water volume injected into each layer, m^3
c	compressibility, $(kgf/cm^2)^{-1}$

References

Abramowitz, M. and Stegun, I. (1964). *Handbook of Mathematical Functions with Formulas, Graphs, and Mathematical Tables*, volume 1. Dover Publications.

Bela, R. V., Pesco, S., and Barreto Jr., A. B. (2019). Modeling falloff tests in multilayer reservoirs. *Journal of Petroleum Science and Engineering*, 174:161–168.

Buckley, S. E. and Leverett, M. C. (1942). Mechanism of fluid displacement in sands. *Transactions of the AIME*, 146:107–116.

Neto, J. L. B., Bela, R. V., Pesco, S., and Barreto Jr., A. B. (2020a). Laplace domain pressure behavior solution for multilayered composite reservoirs. *Paper presented at SPE Latin American and Caribbean Petroleum Engineering Conference (LACPEC)*, July:1–21.

Neto, J. L. B., Bela, R. V., Pesco, S., and Barreto Jr., A. B. (2020b). Pressure behavior during injectivity tests - a composite reservoir approach. *Paper presented at SPE Latin American and Caribbean Petroleum Engineering Conference (LACPEC)*, July:1–20.

Nie, R.-S., Guo, J.-C., Jia, Y.-L., Zhu, S.-Q., Rao, Z., and Zhang, C.-G. (2011). New modelling of transient well test and rate decline analysis for a horizontal well in a multiple-zone reservoir. *Journal of Geophysics and Engineering*, 8:464–476.

Nie, R.-S., Meng, Y.-F., Jia, Y.-L., Zhang, F.-X., Yang, X.-T., and Niu, X.-N. (2012). Dual porosity and dual permeability modeling of horizontal well in naturally fractured reservoir. *Transport in Porous Media*, 92:213–235.

Stehfest, H. (1970). Numerical inversion of laplace transforms. *34th Communications of the ACM*, 13:47–49.

von Hohendorff Filho, J. C. (2004). *IMEX 2003 Básico - Manual Técnico*, volume 1. Petrobras.